Spectroscopic and Electrochemical Studies on the Binding of Pyrocatechol Violet with Telomere DNA and Its Application

Yuanyuan Jiang[1], Ye Yuan[2], Kun Wang[1], Huihui Li[1,**], Chongzheng Xu[1], Xiaodi Yang[1,*]

[1]Jiangsu Key Laboratory of New Power Batteries, School of Chemistry and Materials Science, Nanjing Normal University, Nanjing 210097, China;
[2] St. Olaf College, Northfield, Minnesota, 55057, USA;
[*]E-mail: yangxiaodi@njnu.edu.cn; huihuili@njnu.edu.cn

The interaction between pyrocatechol violet (PCV) and telomere DNA was studied in physiological buffer (pH 7.4) by spectroscopic and electrochemical methods. These results indicated that PCV could bind strongly to the telomere DNA and the major binding mode was intercalative. Based on the voltammetric titration, the binding constant (β) and binding ration (m) of PCV and telomere DNA were found to be 5.3×10^9 mol L^{-1} and 1.7, respectively. The reduction of the peak current of PCV after adding telomere DNA was further used for the quantification of telomere DNA by Differential pulse voltammetry (DPV). The linear range for telomere DNA was in the range of 0.2 -13.0 μmol L^{-1} with the linear regression equation as ΔI_{pa}(μA) = 0.075 (μmol L^{-1})-0.041 and the detection limit of 0.1 μmol L^{-1}. The determination of telomere DNA was hardly impacted by foreign substances.

1. INTRODUCTION

Telomeres can be considered as protective caps for chromosomes, composed of repeated DNA sequences, which is bounded by a series of specialized telomere proteins [1]. They possess the essential nucleoprotein structures and are located at the ends of all eukaryotic chromosomes, will protect the ends of chromosome from degradation and inadvertent recognition when DNA double-strand breaks. During the replication of chromosomes, conventional DNA polymerases cannot fully replicate the ends of chromosomes. Hence telomeres get shorten every cell-cycle [2]. For telomeres in normal dividing cells, progressive shortening eventually results in the loss of end protection, even no cognitive ends of chromosome. Such protection ensures chromosomes' retaining and properly inheriting in cell division. Besides, the loss of entire telomere ends triggers the cell-cycle's rest and, in

mammalian cells, the initiation of cellular senescence, a state halting the progressive replication-associated loss of terminal DNA sequences [3]. However, DNA can be damaged by several physical treatments and chemical reagents, such as UV light ionizing radiation, and photoexcited dyes, leading to the harmful mutations, cell death and cancer [4].

Pyrocatechol violet (PCV), a cationic dye from triphenylmethane family, is usually used to determination of Aluminum (Al) and other metal ions [5, 6]. Its structure is shown by scheme 1. PCV possesses π-π conjugated bond, which has better conductivity with a great amount of active sites [7]. The previous study showed that the poly (PCV) film modified electrodes had good electrocatalytic activity towards redox of small molecular compounds, like ascorbic acid, dopamine [8], hydrazine [9], H_2O_2 [10], NADH [11], etc. However, PCV, as triphenylmethane dye series, also has potential of carcinogenicity, mutagenity and teratogenicity [12-15]. Additionally, DNA is often considered as the target for many tumorigenic and mutagenic molecules [16, 17]. Considering all the facts above, studies on dyes-DNA interaction have attracted lots of interests, which are also considered as the key to designing DNA-target drugs [18-20]. Therefore, the research about PCV's binding to telomere DNA can help to understand the reacting mechanism electrochemically and thermodynamically on molecular level, which can further contribute to designing new effective DNA-targeted anticancer drugs for carcinogenicity.
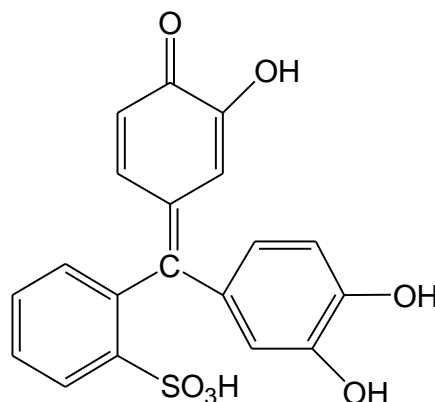
Scheme1. The structure of pyrocatechol violet

Small molecules react with DNA via covalent and noncovalent interactions, while most studies focus on the latter one. The binding of small molecules to DNA occurs mainly through three modes [21]: electrostatic interactions with the negatively-charged nucleic sugar–phosphate structure, binding interactions with the two grooves of the DNA double helix, and intercalation between the stacked base pairs of native DNA. Among these three modes, the intercalative binding is stronger than the other two, because the surface of intercalative molecule is sandwiched between the aromatic heterocyclic base pairs of DNA.

In this research, the mutagenity mechanism of the interaction between PCV and telomere DNA was studied on the biomolecular level. Although there are some previous researches on the interaction between PCV and metal, no much attention is paid to the spectrophotometric and electrochemical aspects about the interacting mechanism between PCV and telomere DNA. Electrochemical methods, including metal complexes [22-24], anticancer or antivirus drugs [25- 28] and organic dyes [29, 30] to

DNA, are often used to investigate the binding of redox substances. The main advantages of the electrochemical methods are simple to conduct and sensitive to detect and direct to study, which are favored by more and more people recently.

2. EXPERIMENTAL

2.1. Apparatus and chemicals

UV-Vis adsorption experiments were carried out on a Cary 5000 probe spectrophotometer (Varian, USA). Fluorescent experiments were measured with LS50B fluorospectrometer (Perkin Elmer, USA). Electrochemical experiments were performed with a CHI660B electrochemical workstation (Chenhua Instrumental, Shanghai, China) using a three-electrode system composed of a glassy carbon electrode (GCE, 3mm diameter) as working electrode, a platinum wire as auxiliary electrode and a saturated calomel electrode (SCE) as reference electrode. Mettler Toledo Seven Multi pH acidimeter (Shanghai Mettler Toledo instrument, China) was used for pH measurement. All the chemical reagents used were of analytical grade. Deionized water was used throughout the entire experiment (Resistance = 18.25 MΩ cm^{-1}).

PCV was provided by Tokyo Chemical Industry Co., Ltd. Special sequences single-stranded telomere DNA was purchased from Sangon Biotech (Shanghai) Co., Ltd. The single-stranded telomere DNA base sequence was as following: ss$_1$: **(5'-TTAGGGTTAGGG-3'); SS$_2$: (5'-CCCTAACCCTAA-3').**

2.2. Procedure

Two special sequences single-stranded telomere DNA were annealed in a water bath at 86 °C for 12 min to obtain steady double-stranded telomere DNA. The double-stranded telomere DNA was dissolved in water or Tris-HCl buffer solution and stored at 4 °C for use. The concentration of double-stranded telomere DNA was determined according to absorbance at 260 nm after establishing the absorbance ratio, (A_{260}/A_{280}) to be in the range of 1.80–1.90. This indicated that the double-stranded telomere DNA was sufficiently free from protein. The molar extinction coefficient, the ε_{260} of double-stranded telomere DNA is taken as 6600 L mol^{-1} cm^{-1}, and single-stranded telomere DNA is 8250 L mol^{-1} cm^{-1} [31]. Denatured single-stranded telomere DNA was produced by heating the double-stranded telomere DNA solution in a water bath at 100 °C for 8 min, immediately followed by rapid cooling in an ice bath for 5 min [32]. PCV dye stock solution (5.00×10^{-3} mol L^{-1}) was prepared by dissolving its powder in doubly distilled water, which diluted to the required volume before use. 0.05 mol L^{-1} Tris-HCl buffer solution containing 0.1 mol L^{-1} NaCl was prepared by dissolving an appropriate amount of tris (hydroxymethyl) −aminomethane and NaCl and then adjusting the pH value with concentrated HCl and NaOH.

Before measurements, the working electrode of GCE was polished successively with fine emery paper and 0.05 μm α-Al$_2$O$_3$ paste on chamois leather pad prior to each series of experiments. Residual polishing materials were removed by ultrasonic cleaning in 95% ethanol and water for 5 min

respectively. The procedures of the electrochemical studies of the interaction of PCV with telomere DNA are as follows: appropriate amounts of telomere DNA, PCV and Tris–HCl buffer were successively added to a colorimetric tube and then transferred to a 10 mL electrochemical cell after reacting for 20 min at ambient temperature to ensure the equilibration. Before the electrochemical experiments, the Tris-HCl buffer solution was degassed for at least 20 min by bubbling high-purity nitrogen gas and the solution was kept in a nitrogen environment to prevent the oxidation. Cyclic voltammetry (CV) was carried out in the range of -1.2 to 1.2 V and Differential pulse voltammetry (DPV) is under taken from -1.0 to 1.0 V with amplitude of 50 mV, pulse width of 50 ms and pulse period of 200 ms.

3. RESULTS AND DISCUSSION

3.1 Spectrophotometric studies

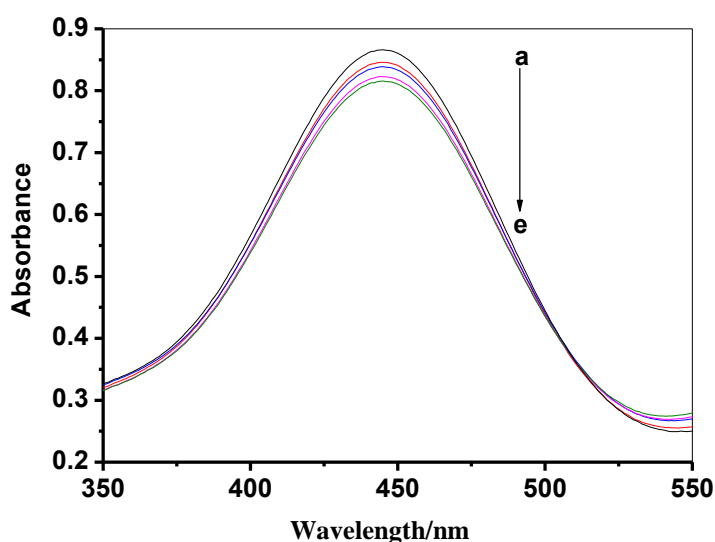*3.1.1.* UV-Vis *absorption spectra of PCV in the presence of double strand telomere DNA*

Figure 1. Absorption spectra of PCV in the presence of telomere DNA at different concentrations. C_{DNA} = 0, 12.5, 24.5, 36.4, 48.0 μmol L^{-1} for curves a-e, respectively, and C_{PCV} = 250.0 μmol L^{-1} in 0.05 mol L^{-1} pH 7.4 Tris-HCl buffer solution (0.1 mol L^{-1} NaCl).

UV-visible absorption spectra were initially used to investigate the interaction between PCV and the telomere DNA [33]. Molecules containing aromatic or phosphate chromophore groups can interact with the double helix structure of DNA. Therefore, the interaction between them can be studied basing on changes of the absorption spectra before and after reaction. As shown in Fig. 1, there is an absorption peak of PCV at 445 nm in the range from 350 to 550 nm in pH 7.4 Tris-HCl buffer solution. Telomere DNA has a maximum absorption at 260 nm (not shown in Fig. 1). After adding telomere DNA to PCV, no new peak appears, while the maximum absorbance at 445 nm has an

evident hypochromic effect. Meanwhile, an isosbestic point between 525 nm and 500 nm provides an evidence for the formation of the new PCV–DNA complex. This observed spectral effects attribute to a strong interaction between the electronic state of the interaction chromphore and of the DNA base [34]. Generally speaking, red shift (or blue shift) and hypochromic (or hyperchromic) effect can be observed in the absorption spectra if molecules intercalate into DNA [35]. Hypochromic effect will be obvious if the intercalation is strong [36]. Therefore, it can be concluded that the binding mode between PCV and telomere DNA is a typical characteristic of intercalation.

3.1.2. Binding and thermodynamic constants with double-reciprocal method

In order to further clarify the interaction mode of PCV with telomere DNA, the binding constant between PCV-DNA at 298K and 313K were calculated according to double-reciprocal equation (1):

$$\frac{A_0}{A - A_0} = \frac{\varepsilon_G}{\varepsilon_{H-G} - \varepsilon_G} + \frac{\varepsilon_G}{\varepsilon_{H-G} - \varepsilon_G} \times \frac{1}{K[DNA]} \quad (1)$$

Where A_0 and A are the absorbances of PCV in the absence and presence of telomere DNA, and ε_G and ε_{H-G} are their absorption coefficients, respectively. The double reciprocal plots of $A_0/(A-A_0)$ versus 1/[DNA] were linear (at 298 and 313K, respectively) and the binding constants were calculated from the ratio of the intercept to the slope equations as 2.10×10^4 and 1.97×10^5 L mol^{-1} at 298 and 313K, respectively (Fig. 2).

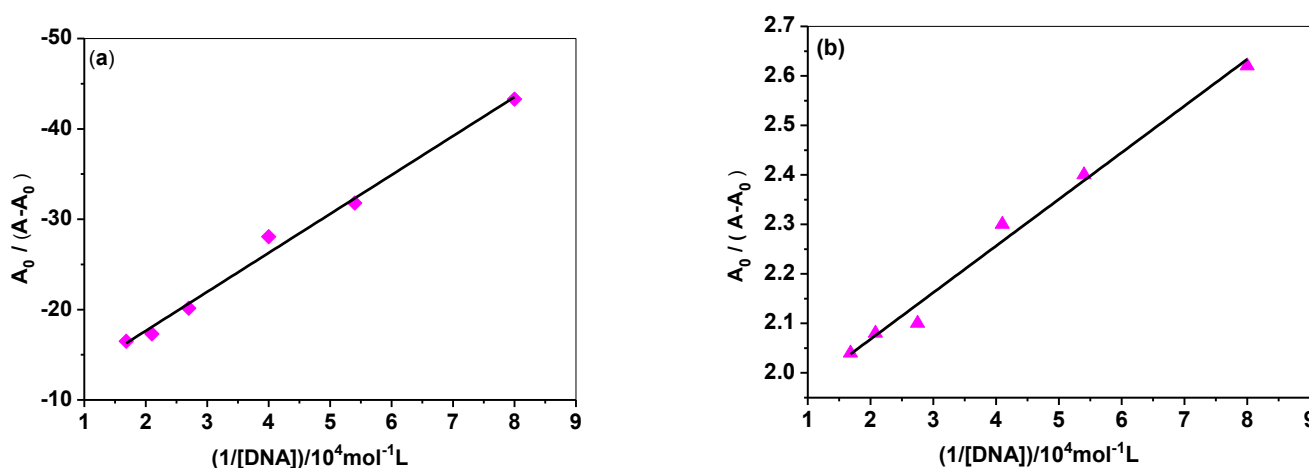**Figure 2.** Plots of $A_0/(A-A_0)$ versus 1/[DNA] for PCV-DNA system at 445 nm in 298 K (a) and 313K (b). Conditions: C_{pcv}=250.0 μmol L^{-1}, C_{DNA}=12.5, 24.5, 36.4, 48.0, 59.5, 81.8 μmol L^{-1} in 0.05 mol L^{-1} pH 7.4 Tris-HCl buffer solution (0.1 mol L^{-1} NaCl).

3.1.3. Thermodynamic parameters and nature of the binding forces

Considering the dependence of binding constant on temperature, a thermodynamic process could be responsible for the formation of a complex. Hence, the thermodynamic parameters dependent on temperatures are analyzed to further characterize the interacting forces between a small molecule and DNA. Small molecules are bound to macromolecules via four binding modes: hydrogen bound, van der Waals, electrostatic, and hydrophobic interactions [37]. To clarify the interaction of PCV with DNA, thermodynamic parameters were calculated from Eqs.2-4. If the temperature does not vary significantly, the enthalpy change (ΔH) can be regarded as a constant. Its value can be evaluated from the Clausius-Clapeyron equation:

$$\ln(\frac{K_2}{K_1}) = -\frac{\Delta H}{R}(\frac{1}{T_2} - \frac{1}{T_1}) \qquad (2)$$

Where R is the gas constant, T is the experimental temperature, and K is the binding constant at the corresponding T. The Gibbs energy change (ΔG) and the entropy change (ΔS) can be obtained from Equations 3 and 4:

$$\Delta G = -RT \ln K \qquad (3)$$

$$\Delta G = \Delta H - T\Delta S \qquad (4)$$

The thermodynamic parameters for the interaction of PCV and telomere DNA are shown in Table 1. According to Table 1, the negative value of ΔG reveals that the interaction process is spontaneous, while $\Delta H>0$ and $\Delta S>0$ associated with the interaction of PCV complex with DNA indicates that the binding is mainly entropy driven and the enthalpy is unfavorable for it (Table 1). In other words, the hydrophobic interaction plays a major role on this binding [38].

Table 1. Binding constants and thermodynamic parameters for the interaction of PCV and telomere DNA

T/K	K/(L·mol^{-1})	ΔH/(J·mol^{-1})	ΔG/(J·mol^{-1})	ΔS/(J·mol^{-1}k^{-1})
298	2.10×10^4	1.16×10^5	-2.47×10^4	472
313	1.97×10^5		-3.17×10^4	

3.1.4. Melting studies

Heat and alkaline environments can destroy the double helix structure of DNA. Thus, the thermal behavior of DNA in the presence of the PCV gives an insight into their conformational changes as well as the information about the interaction strength of PCV with telomere DNA. Helix melting was conducted by recording the DNA absorbance at 260 nm as a function of temperature from

25 to 90 °C. As the temperature of the solution increases, the double stranded DNA dissociates to single strands, generating a hyperchromic effect in the absorption spectra of DNA bases.
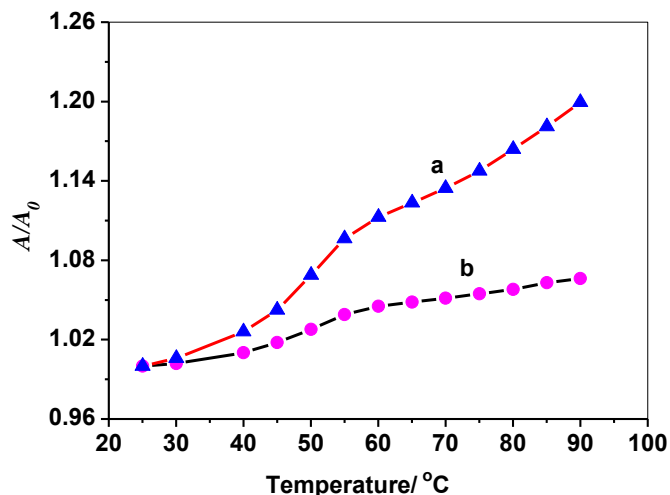

Figure 3. Melting curves of telomere DNA in the absence (curve a) and the presence (curve b) of PCV in 0.05 mol L^{-1} pH 7.4 Tris-HCl buffer solution (0.1 mol L^{-1} NaCl).

This transition of double stranded DNA to single stranded DNA is denoted as the melting temperature (T_m) of DNA. It can be observed that intercalation binding can stabilize the molecular structure and T_m increases by about 5-8 °C, while the non-intercalation binding causes no obvious increase in T_m [39]. The melting curves of DNA in the absence and presence of complexes (curve a) and (curve b) are given in Fig. 3. The T_m of DNA in the absence of PCV is 50 °C under our experimental conditions, while it rises to about 55 °C in the presence of PCV. Therefore, the interaction between PCV and telomere DNA causes the increasing of T_m, suggesting the binding of PCV with telomere DNA should be an intercalation binding.

3.1.5. Fluorescence spectra

Fig. 4 displays the fluorescence spectra of 250.0 μmol L^{-1} PCV with different concentrations of telomere DNA in 0.05 mol L^{-1} Tris-HCl buffer solution (pH 7.4). The fluorescence intensity increases markedly with increasing the concentration of telomere DNA from Fig. 4. The stronger enhancement in fluorescence intensity may be mainly due to the increase of the molecular planarity of the complex and the decrease of the collision frequency of the solvent molecules with the molecule, which is caused by the diffusion between adjacent base pairs of DNA [33]. The increase in the PCV-DNA complex planarity and the decrease in the collision frequency of solvent molecules with PCV usually lead to the enhancement of the PCV fluorescence emission, which also agrees with observations for other intercalators [40-42]. Meanwhile, such enhancement could be found in pH 6.5 and 8.5 solutions as the same as pH 7.4 conditions.
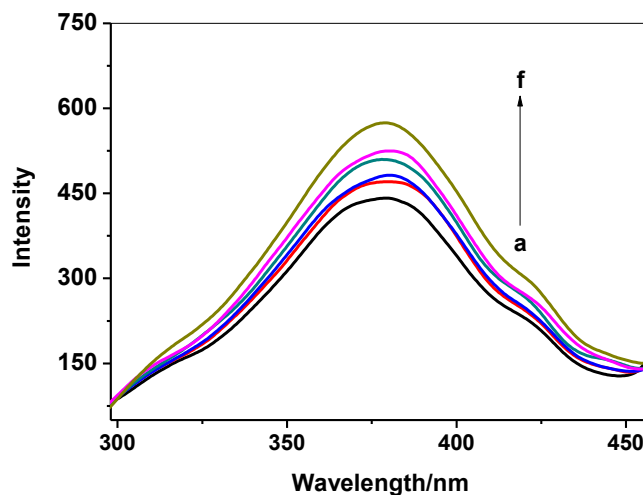
Figure 4. Fluorescence spectra of PCV in the absence and presence of DNA at C_{DNA} = 0, 12.5, 36.4, 48.0, 59.5, 70.8 μmol L^{-1} for curve a-f, respectively, and C_{PCV}= 250.0 μmol L^{-1} in 0.05 mol L^{-1} pH 7.4 Tris-HCl buffer solution (0.1 mol L^{-1} NaCl).

3.2. Electrochemical Characterizations of PCV interacting with double strand telomere DNA

3.2.1 Cyclic Voltammetry

Fig. 5 represents the cyclic voltammograms of PCV and its mixture with telomere DNA. Fig. 5c reveals that telomere DNA is non-electroactive in Tris-HCl buffer solution. However, PCV has three redox peaks in the potential range from -1.2 to 1.2 V at the scan rate of 0.05 Vs^{-1} with two oxidative peaks at 0.232 V (P_1), 0.652 V (P_2) and a reductive peak at -0.777 V (P_3) respectively in Fig. 5a. These peak positions are close to that reported in pH 9.2 phosphate buffer solutions [43]. Potentials of these three peaks do change in the pH range between 6.5 and 8.5, indicating protons involve in the electrode reaction. The ratio of the oxidation peak current (I_{pa}) to the reduction peak current (I_{pc}) is less than one unit, suggesting that the electrochemical process of PCV is irreversible. Throughout the experiments on these systems, the oxidation peak (P_2) is more sensitive and reproducible than that of the reduction peak (P_3) and oxidation peak (P_1). Thus, the oxidation peak (P_2) is chosen as the analysis signal for further studies.

Additionally, for an irreversible reduction process, the number of electron transfer (n) could be obtained by Eq. (5) [44]:

$$| E_{pa} - E_{pa/2} | = 1.857 RT / \alpha n F \quad (5)$$

Where $E_{pa/2}$ is the half peak potential, α represents the electron transfer coefficient (generally, $0.3 < \alpha < 0.7$), F denotes the Faraday constant (96487 Coulombs mol^{-1}), R is the universal gas constant (8.314 J K^{-1} mol^{-1}), T is Kelvin temperature (K). α is assumed to be 0.5 for a totally irreversible process. In this presented study, a value of 56 mV for $|E_{pa}-E_{pa/2}|$ is obtained from Fig. 5 and the value

of n of 1.7($\approx$2) is yielded referring to Eq. (5) [44]. So, the electrochemical oxidation of PCV undergoes $2e^-$ transfer process.
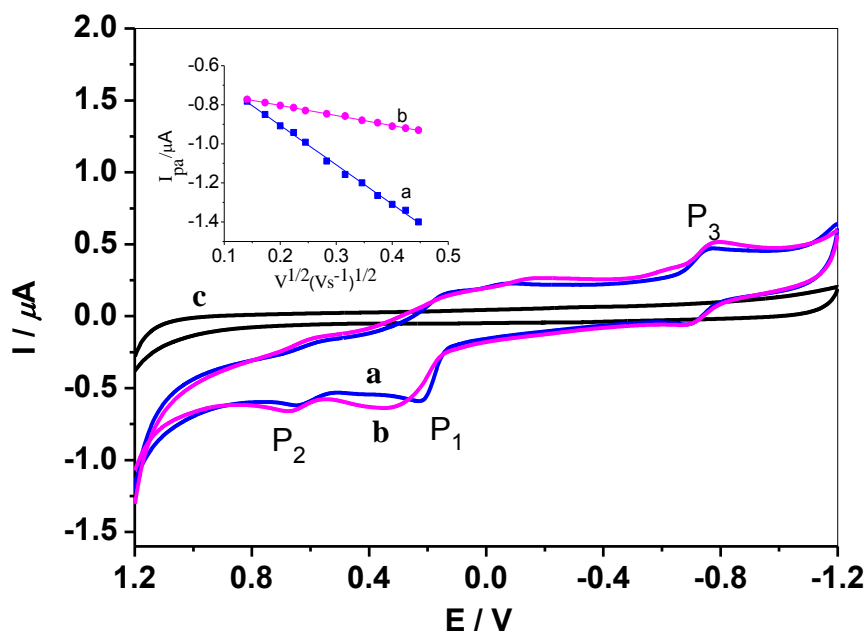

Figure 5. Cyclic voltammograms of 250.0 μmol L^{-1} PCV without (a), with 14.0 μmol L^{-1} telomere DNA (b) and cyclic voltammograms of 14.0 μmol L^{-1} telomere DNA (c) in 0.05 mol L^{-1} pH 7.4 Tris-HCl buffer solution (0.1 mol L^{-1} NaCl). Insert: Plots of I_{pa} versus $v^{1/2}$ for PCV (a) and PCV-DNA complex (b).

According to Galus and Adams' reports concerning the electrochemical behaviors of triphenylmethane dyes such as crystal violet, brilliant green, malachite green and so on [45, 46], the first oxidation peak (P_1) is due to the oxidation of hydrated form and the second oxidative peak (P_2) to the oxidation of the unhydrated form of PCV. The reduction peak (P_3) is the reduction of quinine–hydroquinone [47]. So, it is possible that PCV has two electrons electrochemical oxidation process happened on the GCE with the equation shown by scheme 2.
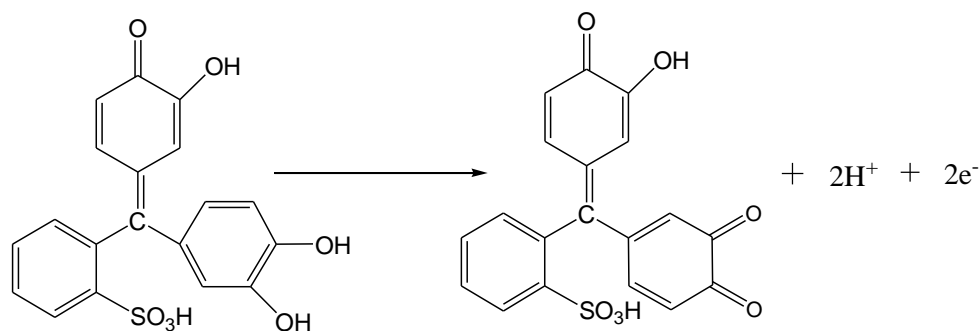
Scheme2. The oxidation process of pyrocatechol violet

After adding 1.25×10^{-3} mol L^{-1} telomere DNA into 250.0 μmol L^{-1} PCV solution and then voltammetrically detected under the same condition, no new redox peak appeared in voltammogram. The oxidation peak current of P_2 decreased dramatically along with a positive shift of the potential (Fig. 5b), suggesting that PCV is bound to telomere DNA via an intercalative mode as well as in pH 8.5 [23]. At the same time, we also find that the oxidation peak current of P_2 declined with more negative shift of the potential, indicating an electrostatic interaction of PCV protonated with the outer negatively charged DNA phosphate in pH 6.5. Bardetal et al. [48] reported the positive shift in peak potential for hydrophobic interactions (for intercalators) and negative shift for electrostatic interactions. Therefore, the positive shift in peak potential of PCV observed in the present work revealed the presence of intercalative mode of binding between telomere DNA and PCV. The acting force is mainly hydrophobic between them, which is consistent with the thermodynamics experiment.

Also, according to the value of $|E_{pa}-E_{pa/2}|$ in Fig. 5 and Eq.(5), the number of electron transfer is calculated to be about 2, suggesting that PCV-DNA complex also undergoes a two electron transfer process. Moreover, the relationship between the peak current and scan rates in the absence and presence of telomere DNA are investigated. In both cases of telomere DNA's presence and absence, the oxidation peak current of P_2 is linearly related to the square root of the scan rate, showing that the electrode process of free PCV and PCV-DNA are controlled by irreversible diffusion [44]. As shown Fig. 5, the regression equations are $I_{pa}/\mu A=-2.02v^{1/2}/(vs^{-1})^{1/2}-0.502(R^2=0.997)$ and $I_{pa}/\mu A=-0.52v^{1/2}/(vs^{-1})^{1/2}-0.7(R^2=0.997)$, for free PCV and PCV-DNA complex. Obviously, the slop of free PCV system is much larger than that of PCV-DNA complex system, suggesting that free PCV diffused more quickly than that of DNA PCV-DNA complex. As the result of the above experiments, the decrease of peak currents of PCV upon adding telomere DNA could be caused by the diffusion of an equilibrium mixture of free and telomere DNA-bound PCV to the electrode surface [44].

The change of electron-transfer rate constant (K_s) of electroactive molecules after interaction with DNA is often used to probe the difference of electrochemical properties between small molecules and their DNA-bound complex DNA [49, 50]. In this work, the K_s of DNA-bound PCV was also determined and then compared with that of free PCV. The plots of the oxidation peak potentials (E_{pa}) of PCV (curve a) and PCV-DNA complex (curve b) with the scan rate (v) are in Fig. 7. The oxidation peak potential (P_2) values increases as the scan rate for both of the systems rises. Then the formal potentials of free and DNA-bound PCV were obtained to be +0.652 V and +0.680 V, via prolonging the $E_{pa}-V$ curves to E_{pa} axis. Additionally, it is observed that E_{pa} is linearly dependent on logarithm of scan rate (ln$V$) for both the systems (Fig. 6), which is in accordance with the following Laviron's Eq. (6)

$$E_{pa} = E_{pa}^{0'} + (RT / \alpha nF)\ln(\alpha nF / RTK_S) + (RT / \alpha nF)\ln V \quad (6)$$

For an irreversible oxidation process [51], the values of K_s are evaluated to be 0.52 s^{-1} in the absence of DNA and 0.54 s^{-1} in presence of DNA according to Eq. (6).
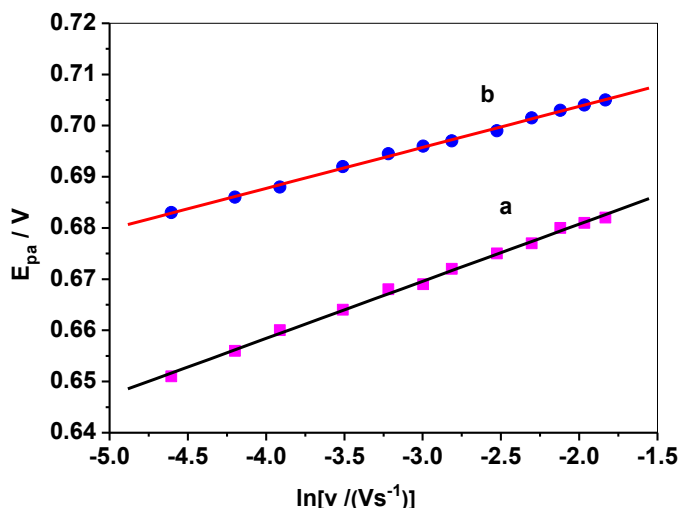
Figure 6. Relationship between the oxidation peak potentials (E_{pa}) and the logarithm of scan rate ($\ln V$).
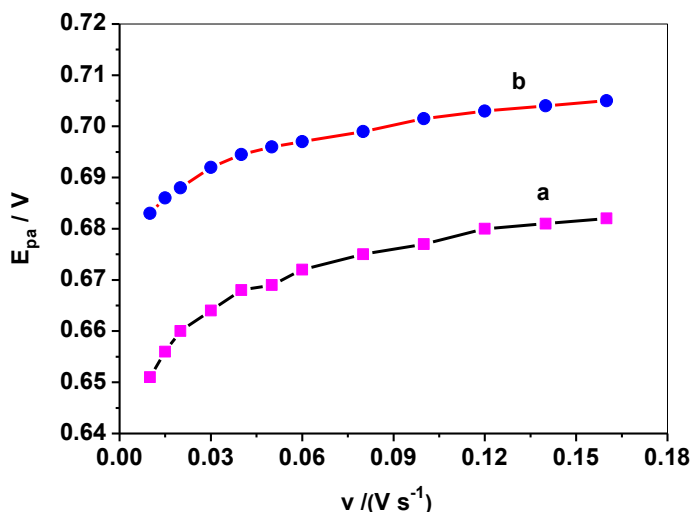

Figure 7. Relationships between the oxidation peak potential (E_{pa}) and the scan rate (v) for PCV (a) and PCV-DNA complex (b).

Since K_s in the absence and presence of telomere DNA are almost same, we propose that the telomere DNA does not alter the electrochemical kinetics of oxidation of PCV [32]. That is to say, PCV-DNA complex still keep the electroactivity of free PCV in homogeneous solution [52].

The decrease in peak current of PCV after being added into telomere DNA may be due to the following two reasons: the first reason could be the electrochemical phenomena, which resulted in the changes of electrochemical parameter such as the surface reaction rate constant (K_s) [32]. The values of K_s is evaluated to be 0.52 s^{-1} and in the absence of telomere DNA and 0.54 s^{-1} in presence of telomere DNA. Since the values K_s in the absence and presence of telomere DNA are almost the same, we propose that the telomere DNA did not alter the electrochemical kinetics of oxidation of PCV and formed complex between PCV and telomere DNA.

Another possibility for decreasing in peak current may be due to the competitive adsorption between PCV and telomere DNA. Since the electrode process of PCV is a diffusion controlled irreversible process and no adsorption time is given in these experiments, the possibility of competitive adsorption between PCV and telomere DNA can be ruled out. It was reported [53] that under the conditions of lower concentration species, larger electrode area and shorter accumulation time, competitive adsorption between PCV and telomere DNA does not exist. In view of the above, the decrease in peak current of PCV upon the addition of telomere DNA is mainly attributed to decrease in equilibrium concentration of free PCV. This decrease in the concentration of PCV could be attributed to the formation of the electrochemically inactive PCV-DNA system, which indicates that the PCV interacts with telomere DNA.

3.2.2 Differential Pulse Voltammetry

Differential pulse voltammetry method (DPV) is chosen for analytical application because it is more sensitive than cyclic voltammetric method. When adding telomere DNA to PCV solution, marked decrease in oxidation peak current of PCV with a large positive shift in peak potential was noticed. Besides, no new oxidation peaks were noticed. This revealed the interaction between telomere DNA and PCV. The interaction of PCV was found to depend on time. In order to find out the interaction time, we recorded the differential pulse voltammogram of PCV in presence of telomere DNA at different time intervals. We observed a significant decrease in peak current of PCV up to 20 min. After 20 min, the peak current of PCV remained almost the same. Therefore, an interaction time of 20 min should be maintained throughout the experiment. Fig. 8 shows the DPV of PCV in the absence (curve a) and presence of excess telomere DNA (curve c). PCV has an oxidation peak at 0.652 V, which was corresponding to the peak of P_2 on the cyclic voltammogram, where the oxidation peak currents of PCV decreases dramatically and the peak potential shifts from 0.652 V to 0.680 V after interacting with telomere DNA. From the previous study [48], it was reported that if both the oxidized and reduced forms of a small molecule interacted with DNA, the corresponding equilibrium constants for each oxidation state binding telomere DNA could be calculated from the following Eq. (7):

$$\Delta E^0 = E_b^{0'} - E_f^{0'} = (\frac{RT}{nF})\ln(K_R / K_0) \qquad (7)$$

Where $E^{0'}{}_b$ and $E^{0'}{}_f$ are the formal potentials for DNA-bound and free forms of PCV, respectively, are determined by the formula of $E^{0'}=E_{pa} + \Delta E_p/2$, ($E_{pa}$, the DPV peak potential; ΔE_p, the pulse amplitude); K_0 and K_R are the binding constants of oxidized and reduced forms to telomere DNA, respectively. Thus, for the limiting potential shift of 28 mV after interacting with excess telomere DNA, the ratio of the binding constants (K_R/K_0) is 8.1 from calculation, indicating that the reduced form of PCV (PCV_{Red}) bound to telomere DNA is 8 times stronger than the oxidation form (PCV_{ox}). This result is consistent with the characteristic of an intercalation mode [48].
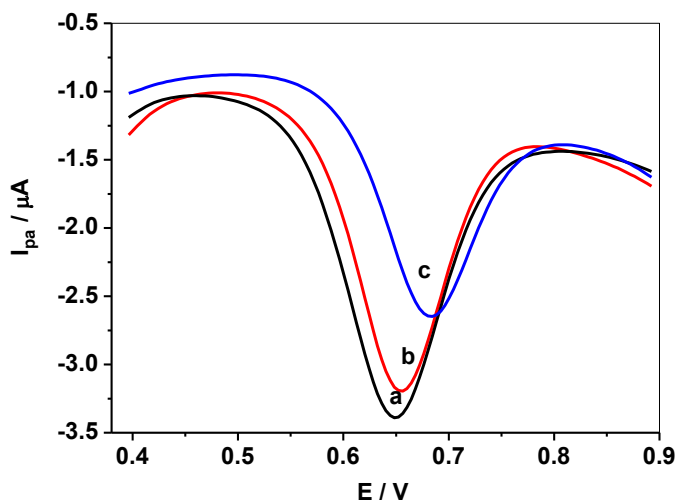
Figure 8. Differential pulse voltammograms of 250.0 μmol L^{-1} PCV in the absence (a) and presence of 14.0 μmol L^{-1} single-stranded telomere DNA (b) and 14.0 μmol L^{-1} double-stranded telomere DNA (c) in a buffer solution of 0.05 mol L^{-1} pH 7.4 Tris-HCl (0.1 mol L^{-1} NaCl).

3.2.3 Comparison of the interaction of PCV-double-stranded telomere DNA with PCV-single-stranded telomere DNA

The binding proposed for the interaction between small molecules and DNA double helix include intercalative binding, groove binding and electrostatic binding. Among these, intercalation and groove binding modes depend on DNA double helix. However, the electrostatic binding occurs out of the groove of the DNA. If the interaction models are intercalative and groove binding, the interacting capability would decrease in presence of denatured DNA. It was found that the interaction between PCV and denatured single-stranded telomere DNA (Fig. 8, curve b), while the obtained signal showed minor change compared with free PCV (Fig. 8, curve a), indicating that the interaction between PCV and denatured telomere DNA is very weak. However, the electrostatic interactions may continue to operate even after DNA's denaturation. After denatured single-stranded telomere DNA's interaction with PCV, the oxidation peak potential shifts negatively. This could be attributed to the electrostatic binding between PCV and negative-charged backbone PO$_2$ group of denatured DNA. For the denatured telomere DNA, the hydrogen bonding between two associated strands is destroyed and the two strands are separated into two "random-coil" states, resulting in the extinction of intercalation sites for the external molecules.

Appreciable decrease in the electrochemical signals after interacting with telomere DNA further supports that the PCV intercalates into double helix of telomere DNA.

Fig. 9 shows the relationship between oxidation peak current (I_{pa}) and concentration of PCV. It is found that in the incipient stage, the oxidation peak (I_{pa}) decreases rapidly with the increase of telomere DNA concentration, and then becomes placid (stable value) when the equilibrium concentration of PCV goes over 14.0 μmol L^{-1}, which suggests a complete interaction of telomere DNA with 250.0 μmol L^{-1} PCV.
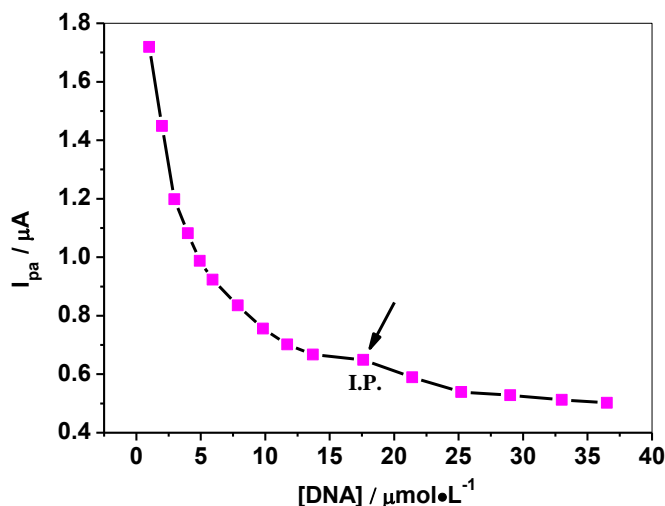
Figure 9. Plot of I_{pa} vs [DNA] for 250.0 μmol L^{-1} PCV with varying concentration of DNA in a buffer solution of 0.05 mol L^{-1} pH 7.4 Tris-HCl (0.1 mol L^{-1} NaCl).

According to reference [27, 48, 54, 55], the binding ratio (*m*) and binding constant (*β*) can be obtained, under the condition of PCV binds telomere DNA to form a simple complex. Assuming that PCV and telomere DNA produce only a single complex of telomere *DNA-mPCV*:
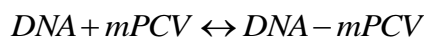
$$DNA + mPCV \leftrightarrow DNA - mPCV$$

The binding constant is

$$\beta = DNA - mPCV / [PCV]^m [DNA]$$

Because

$$[DNA] = C_{DNA} - [DNA - mPCV]$$

$$\Delta I_{Pa,\max} = KC_{DNA}$$

$$\Delta I_{Pa} = K[DNA - mPCV]$$

Therefore

$$\Delta I_{Pa,\max} - \Delta I_{Pa} = K[DNA]$$

And the following equations can be deduced

$$\lg[\Delta I_{Pa} / \Delta I_{Pa,\max} - \Delta I_{Pa})] = \lg \beta + m \lg[PCV]$$

Or $\quad\quad\quad 1/\Delta I_{Pa} = 1/\Delta I_{Pa,\max} + (1/\beta\Delta I_{Pa,\max})(1/[PCV]^{m})$

Where ΔI_{pa} represents the oxidation peak current differences with and without telomere DNA, $\Delta I_{pa,max}$ corresponds to the maximum difference of the peak currents before and after the addition of telomere DNA. C_{pcv} and $[PCV]$ correspond to the concentration added and the equilibrium concentration of PCV. If telomere DNA and PCV form a single complex, the plot of $lg[\Delta I_{pa}/(\Delta I_{pa,max}-\Delta I_{pa})]$ versus $lg[PCV]$ is linear. Fig. 10 shows that $lg[\Delta I_{pa}/(\Delta I_{pa,max}-\Delta I_{pa})]$ depends on $lg[PCV]$, with a fine straight line. From the slope and the intercept of the straight line, the values of m and β can be acquired as 1.7 and 5.3×10^{9} mol L^{-1}. A tentative idea was that the binding ratio of telomere DNA and PCV was 1: 2.
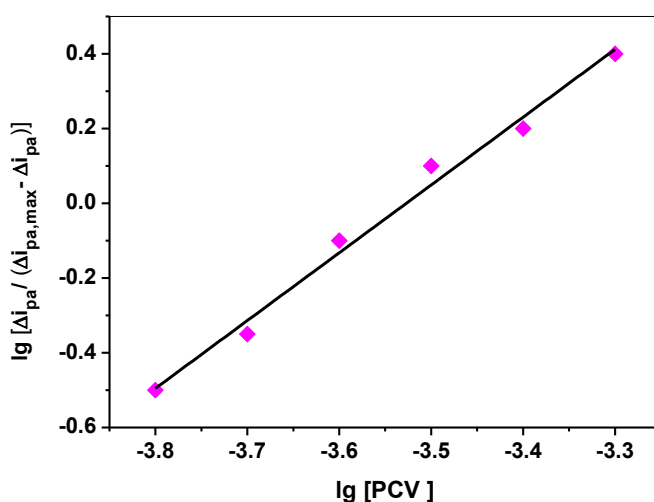

Figure 10. The plot of $lg[\Delta I_{pa}/(\Delta I_{pa,max}-\Delta I_{pa})]$ versus $lg[PCV]$.

3.3 The influence of ionic strength on interaction of PCV and telomere DNA

The effect of the ionic strength controlled by adding NaCl on the interaction of PCV and telomere DNA are also studied. It is found that in the range of 0-0.3 mol L^{-1}, the oxidation peak potential of PCV shifts positively when increasing ionic strength. This evidence suggests that adding NaCl weakens the electrostatic interaction between PCV and telomere DNA [23]. The explanation can be the ionic strength shielding effect of the added Na^{+} on the outer negatively charged DNA phosphate. When I goes beyond 0.1 mol L^{-1}, the oxidation peak potential becomes approximately constant, which indicates that PCV can no longer interact with DNA electrostatically at high ionic strength. The dash line in Fig. 11 divides the binding mode of PCV and telomere DNA into two parts: the mixture of electrostatic and intercalative modes ($I < 0.1$ mol L^{-1}) and the only intercalative mode ($I \geq 0.1$ mol L^{-1}) .
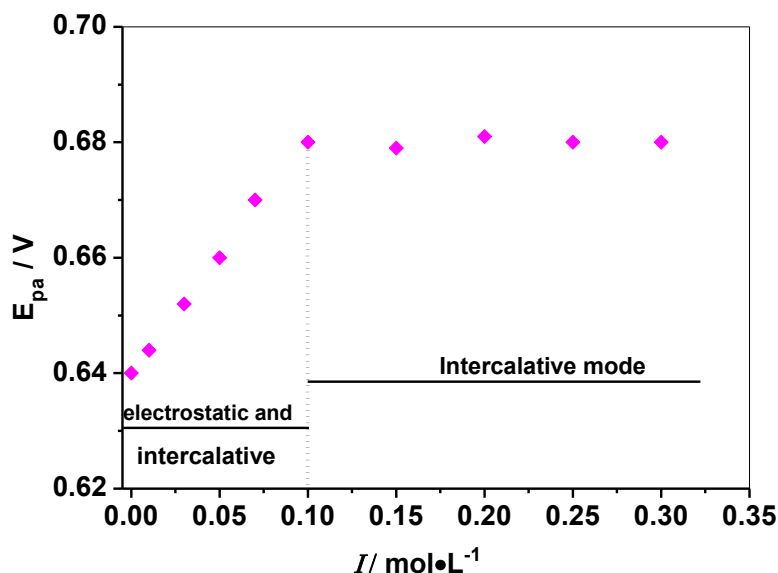
Figure 11. Effect of ionic strength (I) on the oxidation peak potential (E_{pa}) of PCV-DNA system.

3.4 Calibration Curve and Detection Limit

Under the optimum condition of the standard procedure, by keeping the concentration of PCV as 250.0 μmol L^{-1}, the calibration curve for detecting telomere DNA was obtained. When the concentration of telomere DNA is in the range of 0.2 to 14.0 μmol L^{-1}, a linear relationship of the decrease of the oxidative peak current (ΔI_{pa}) with telomere DNA concentration (C) was obtained with a linear regression equation ΔI_{pa}(μA) = 0.0751C (μmol L^{-1})-0.0410, R^2=0.9922 (Fig. 12), providing a possibility for quantitative determination of telomere DNA via using PCV an electroactive probe. The detection limit (*3σ*) was 0.1 μmol L^{-1}, where σ was the standard deviation of the blank measurements (n=10).
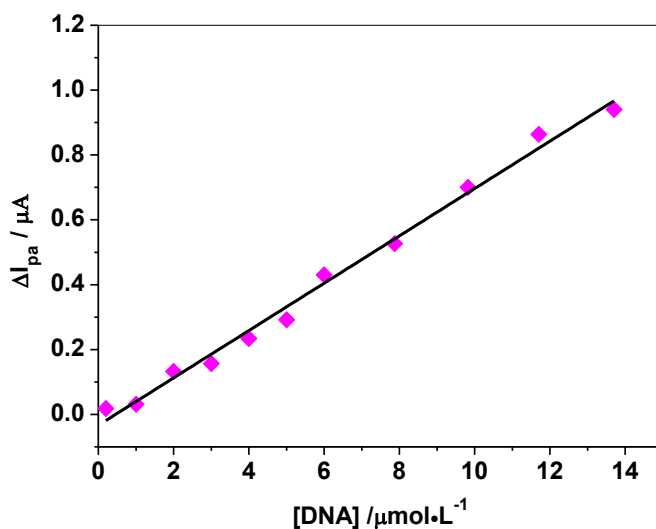

Figure12. Plot of ΔI_{pa} vs [DNA] for 250.0 μmol L^{-1} PCV with varying concentration of DNA in a buffer solution of 0.05 mol L^{-1} pH 7.4 Tris-HCl (0.1 mol L^{-1} NaCl).

3.5. Interference test of foreign substances

Maintaining the concentration of telomere DNA as 1.2×10^{-5} mol L^{-1}, the interference of foreign substances such as some amino acids, glutathione, sodium glutamate and various cations at pH 7.4 on the determination of telomere DNA were tested according to the standards procedure. The results are shown in Table 2. Therefore we conclude that the determination of telomere DNA is hardly impacted, which shows that the interaction of PCV and telomere DNA provides a possibility for detecting the content of telomere DNA in practical samples.

Table 2. Effect of coexisting substances on the determination of 1.2×10^{-5} mol L^{-1} telomere DNA.PCV (250.0 μmol L^{-1}), pH 7.4.

Coexisting Substance	Concentration (μg/ml)	Relative error ($\Delta i_p\%$)	Coexisting Substance	Concentration (μmol/L)	Relative error ($\Delta i_p\%$)
L-Aspartic acid	10	2.14	Cu^{2+}	10	-2.47
L-Serine	10	3.75	Fe^{3+}	10	-6.44
Glutathione	10	-0.81	Mg^{2+}	10	3.05
Citric acid	10	5.93	Ca^{2+}	10	2.17
Sodium Glutamate	10	-4.56	Zn^{2+}	10	4.23

4. CONCLUSION

In this research, the interaction of PCV with telomere DNA was studied by electrochemical and spectroscopic methods. The binding of PCV to telomere DNA resulted in a series of changes in the electrochemical behavior and spectra characteristics. Upon binding to telomere DNA, the adsorption spectra of PCV showed peculiar hypochromic effect and the fluorescence emission of PCV efficiently increased due to the decrease of the collision frequency of the solvent molecules. Meanwhile, the melting temperature of the solution containing PCV increased in the presence of telomere DNA. Moreover, we also found that the irreversible oxidation peak of the PCV was observed decreasing and underwent a positive shift of potential. From these experimental results, it could be affirmed that the interaction of PCV with telomere DNA was intercalative mode. The intercalation caused changes in the shape of the DNA helix and hindered DNA replication and RNA transcription [56]. Furthermore, The results of the CV study showed that the interaction was mainly of an electrostatic one in Tris-HCl buffer solution at pH 6.5 in lower ionic strength, whereas intercalative binding and hydrophobic force played dominant role at pH 8.5 and 7.4 in ($I \geq 0.1$ mol L^{-1}) Tris-HCl buffer solution. These investigations indicated that electrochemistry coupling with spectroscopy techniques could provide a convenient way to characterize both the binding mode and the intercalation mechanism of PCV binding to telomere DNA, which was important for the mechanism of mutagenity and the design of new effective anticancer drugs.

References

1. T.DeLange, V. Lundblad and E. Blackburn E, *Telomeres, 2nd edn*. Cold Spring Harbor Laboratory Press, New York (2006).
2. X. R. Wang and P. Baumann, Cell Press, Kansas (2008).
3. J.A. Stewart, M. F. Chaiken, F. Wang and C. M. Price, *Muta. Rese*., 730 (2012) 12.
4. E. Palecek and M. Fojta, *Anal. Chem*., 73 (2001) 74.
5. I. Narin, M. Tuzen and M. Soylak, *Talanta*, 63 (2004) 411.
6. O. Domínguez and M. J. Acros, *Electroanalysis*, 12 (2000) 449.
7. X. Hu, K. Jiao, W. Sun and J. Y. You, *Electroanalysis*, 18 (2006) 613.
8. C. X. Cai and K. H. Xue, *Microchem*. J., 61 (1999) 183.
9. S. M. Golabi, H. R. Zare and M. Hamzehloo, *Microchem*. J., 69 (2001) 111.
10. Q. L. Sheng, H. Yu and J. B. Zheng, *Electrochim. Acta*., 52 (2007) 7300.
11. S. M. Golabi, H. R. Zare and M. Hamzehloo, *Electroanalysis*, 14 (2002) 611.
12. S. J. Clup and F. A. Beland, *J. Am. Coll. Toxicol*., 15 (1996) 219.
13. S. J. Culp, F. A. Beland, R. H. Heflich, R. W. Benson, L. R. Blankenship and P. J. Webbl, *Muta. Res*., 506 (2002) 55.
14. V. Fessard, T. Godard, S. Huert, A. Mourot and J. M. Poul, *J. Appl. Toxicol*., 19 (1999) 421.
15. K. Mitrowska and A. Posyniak, *Bull Vet Inst Pulawy*, 48 (2004) 173.
16. M. Wainwright, *Dyes and Pigments*, 76 (2008) 582.
17. T. Pecere, M. V. Gazzola and C. Mucignat, *Cancer Res*., 60 (2000) 2800.
18. B. K. Sahoo, K. S. Ghosh. R. Bera and S. Dasgupta, *Chem. Phys*., 351 (2008) 163.
19. Y. T. Sun, S. Y. Bi, D. Q. Song, C. Y. Qiao, D. Mu and H. Q. Zhang, *Sens. Actuators. B. Chem*., 129 (2008) 799.
20. X. Ling, W. Y. Zhong, Q. Huang and K. Y. Ni, J. Photochem. *Photobiol. B. Biol*., 93 (2008) 172.
21. A. M. Pyle, J. P. Rehmann, R. Meshoyrer, C. V. Kumar, N. J. Turro and J. K. Barton, *J. Am. Chem. Soc*., 111 (1989) 3051.
22. M. T. Carter and A. J. Bard, *J. Am. Chem. Soc*., 109 (1987) 7528.
23. M. T. Carter, M. Rodriguez and A. J. Bard, *J. Am. Chem. Soc*., 111(1989) 8901.
24. D. W. Pang and H. D. Abruna, *Anal. Chem*., 70 (1998) 3162.
25. J. Wang, M. Ozsoz, X. H. Cai and G. Rivas, *Bioelectro-chem Bioenerg*, 45 (1998) 33.
26. M. S. Ibrahim, *Anal. Chim. Acta*., 443 (2001) 63.
27. Q. Feng, N. Q. Li and Y. Y. Jiang, *Anal. Chem. Acta*., 344 (1997) 97.
28. Z. W. Zhu, C. Li, N. Q. Li, *Microchem. J.*, 71 (2002) 57.
29. K. Jiao, Q. J. Li, W. Sun and Z. J. Wang, *Electroanalysis*, 17 (2005) 997.
30. M. S. Ibrahim, M. Mkamal and Y. M. Temerk, *Anal. Bioanal. Chem*., 375 (2003) 1024.
31. M. E. Reichman, S. A. Rice, C. A. Thomas and P. Doty, *J. Am. Chem. Soc.*, 76 (1954) 3047.
32. S. S. Kalanur, J. Seetharamappa and S. N. Prashanth, *Colloids and Surfaces*, 82 (2011) 438.
33. R. Hajian and M. Zafari, *Chin. J. Chem*., 29 (2011) 1353.
34. E. C. Long and J. K. Barton, *Acc. Chem. Res.*, 23 (1990) 271.
35. S. A. Tysoe, R. J. Morgan, T. C. Baker and T. C. Strekas, *J. Phys.Chem*., 97 (1993) 1707.
36. E. J. Gao, S. M. Zhao, Q. T. Liu and R. Xu, *Acta. Chimica. Sinica*., 62 (2004) 593.
37. N. Barbero, E. Barni, C. Barolo, P. Quagliotto, G. Viscardi, L. Napione, S. Pavan and F. Bussolino, *Dyes and Pigments*, 80 (2009) 307.
38. D. P. Ross and S. Subramanian, *Biochemistry*, 20 (1981) 3096.

39. C. V. Kumar, R. S. Turner and E. H. Asuncion, *J. Photochem. Photobiol. A. Chem*., 74 (1993) 231.
40. J. K. Barton, J. M. Goldberg, C. V. Kumar and N. J. Turro, *J. Am. Chem. Soc.,* 108 (1986) 2081.
41. Y. Ni, S. Du and S. Kokot, *Anal. Chim. Acta*., 584 (2007) 19.
42. A. A. Ensafi, R. Hajian and S. J. Ebrahimi, *Braz. Chem. Soc*., 20 (2009) 266.
43. Y. Wang, *Colloids and Surfaces*, 88 (2011) 614.
44. A. J. Bard and L. R. Faulkner, *Electrochemical methods: fundamentals and applications, 2nd ed,*. wiley: NewYork (1980)**.**
45. Z. Galus and R. N. Adams, *J. Am. Chem. Soc*., 84 (1962) 3207.
46. Z. Galus and R. N. Adams, *J. Am. Chem. Soc*., 86 (1964) 1666.
47. Q. L. Sheng, H. Yu and J. B. Zheng, *Electrochimica. Acta*., 52 (2007) 7300.
48. Q. X. Wang, X. L. Wang, Z. L. Yu, X. L. Yuan and K. Jiao, *Int. J. Electrochem. Sci*., 6 (2011) 5470.
49. K. Jiao, Q. J. Li, W. Sun and Z. Y. Wang, *Chem. Res. Chin. Univ*., 21 (2005) 145.
50. Q. X. Wang, K. Jiao, F. Q. Liu, X. L. Yuan and W. J. Sun, *Biochem. Biophys. Methods*, 70 (2007) 427.
51. E. Laviron, *J. Electroanal. Chem*., 10 (1979) 19.
52. Q. X. Wang, F. GAO and X. L. Yuan, *Dyes and Pigments*, 84 (2010) 213.
53. Z. Zhu, C. Li, and N. Q. Li, *Microchem. J.,* 71 (2002) 57.
54. X. Bai, K. Jiao, W. Sun and X. Zhang, *Int. J. Electrochem. Sci*., 2(2007) 406.
55. K. Zhang, W. Liu, *Int. J. Electrochem. Sci.*, 6 (2011) 1669.
56. J. W. Lown, S. K. Sim and K. C. Majumdar, Biochem. *Biophys. Res. Commun*., 76 (1997) 705.